Biosensors and Bioelectronics 41 (2013) 446–451

Contents lists available at SciVerse ScienceDirect

Biosensors and Bioelectronics

journal homepage: www.elsevier.com/locate/bios

Anti-EpCAM modified LC-SPDP monolayer on gold microelectrode based electrochemical biosensor for MCF-7 cells detection

Sunil K. Arya*, Karen Yanping Wang, Chee Chung Wong, Abdur Rub Abdur Rahman

*Bioelectronics Program, Institute of Microelectronics, A*STAR (Agency for Science, Technology and Research), 11 Science Park Road, Singapore Science Park II, Singapore 117685, Singapore*

ARTICLE INFO

Article history:
Received 19 July 2012
Received in revised form
27 August 2012
Accepted 5 September 2012
Available online 13 September 2012

Keywords:
Breast cancer
MCF-7 cells
Molecular profiling
Magnetic beads enhancement
Redox tagging
Self-assembled monolayer

ABSTRACT

A succinimidyl 6-(3-[2-pyridyldithio]-propionamido) hexanoate (LC-SPDP) self-assembled monolayer (SAM) prepared onto a 500 μm (diameter) gold microelectrode (Au) surface has been utilized for covalent immobilization of anti-EpCAM antibody. Amino group on anti-EpCAM antibody was covalently bound with succinimidyl group on SAM via amide bond and unreacted active groups of LC-SPDP were blocked using 1% ethanol amine (EA). These anti-EpCAM/LC-SPDP/Au electrodes were characterized using cyclic voltammetric (CV) and fluorescence techniques, respectively. The anti-EpCAM/LC-SPDP/Au electrodes were exposed to solutions with different MCF-7 cell concentrations and CV technique was used to determine the cell concentration. Further, CV studies on blank 500 and 50 μm (diameter) gold microelectrodes were used to identify cell via molecular profiling using ferrocene amidopentyl carboxylic acid based redox tagging and magnetic beads based enhancement. CV results confirm that the anti-EpCAM/LC-SPDP/Au based biosensor could detect MCF-7 cells in the range of 1×10^5–1×10^8 with correlation coefficient of 0.999 and detection limit of 1×10^5 cells ml^{-1} i.e. 100 cells in solution used for incubation (1 μl). Molecular profiling studies suggest that smaller size microelectrode (50 μm; diameter) with magnetic beads based enhancement can be employed to identify cell type. This work establishes the feasibility of using microelectrode based platform for breast cancer specific MCF-7 cell concentration estimation and their molecular profiling.

1. Introduction

Breast cancer is one of the most frequently diagnosed cancer among women globally and its distant metastases is regarded as the major cause of mortality (Amadori et al., 2009; Krishnamurthy et al., 2010; Li et al., 2010; Riethdorf et al., 2007). Breast cancer is known to shed tumor cells into the circulation at the earliest stages of primary tumor development and it is accepted that early stage detection of breast cancer cells could decide the patient's fate (Cristofanilli et al., 2004; Gaforio et al., 2003; Ross and Slodkowska, 2009; Zheng et al., 2011a). Further, it has been shown that their precise estimation in blood will provide the most appropriate approach, for more reliable and effective diagnosis of cancer stage (Adams et al., 2008; Braun and Marth, 2004; Cristofanilli et al., 2004; De Bono et al., 2008; Mostert et al., 2009; Pantel and Riethdorf, 2009; Ring et al., 2004; Slade and Coombes, 2007). Thus, their detection and quantification at early stage are necessitating the development of new and reliable techniques.

Presently majority of the methodologies for detection and estimation of pre-enriched tumor cells via various protocols (Hosokawa et al., 2010; Issadore et al., 2011; Lin et al., 2010; Moon et al., 2011; Sequist et al., 2009; Zborowski and Chalmers, 2011; Zheng et al., 2011a, b) uses RT-PCR and/or optical fluorescence to identify cytoskeletal and nuclear markers (Alunni-Fabbroni and Sandri, 2010; Hosokawa et al., 2010; Kuo et al., 2010; Lin et al., 2010; Mostert et al., 2009; Sun et al., 2011; Tan et al., 2009; Zborowski and Chalmers, 2011; Zheng et al., 2011a, b). Although, these methods have the advantage of being quite mature and well established, they are labor intensive, costly, time consuming, and suffer from operator variance (Miller et al., 2010). Therefore, there is a need for alternate rapid, sensitive, and affordable cancer cell detection platforms. Recently, electrochemical techniques based biosensor/ detection system have gained much attention for cancer cell detection as they provide easy operation, accuracy, selectivity, and sensitivity even at single cell level (Chung et al., 2011; De la Rica et al., 2009; Li et al., 2010). Further, electrochemical techniques such as cyclic voltametry can be employed for molecular profiling of cell using redox tagged antibody or nanomaterials. Recently, Li et al. have described the electrochemical immunosensor with signal amplification for detection of cancer marker using ferrocene functionalized iron oxide nanoparticles (Fe_3O_4). Using dopamine functionalized Fe_3O_4 conjugated to ferrocene carboxylic acid and secondary antibody, they achieved detection upto 2 pg ml^{-1} of prostate specific antigen (Li et al., 2011). In last few years, electrochemical transduction based detection on microelectrodes has gained

* Corresponding author. Tel.: +65 90702464; fax: +65 64640517.
E-mail address: sunilarya333@gmail.com (S.K. Arya).

0956-5663/$ - see front matter © 2012 Elsevier B.V. All rights reserved.
http://dx.doi.org/10.1016/j.bios.2012.09.006

much attention for detection of cells with higher sensitivity (Arya et al., 2012; Davies and Compton, 2005; Ordeig et al., 2006; Rahman and Guiseppi-Elie, 2009; Rahman et al., 2009). Microelectrodes offer several benefits over larger area macroelectrodes such as higher sensitivity with minimum variability due to higher radial diffusion profile as opposed to a planar diffusion profile in macroelectrodes. Thus, microelectrodes are desirable for applications such as in rare cell detection, wherein higher resolution is required.

In biosensor fabrication selection of a proper matrix for binding of recognition molecule such as antibody or enzyme is known to play a crucial role. Recently, self-assembled monolayers (SAMs) have attracted increasing attention as a potential candidate for electrode fabrication by immobilizing biomolecules such as enzymes, DNA, and antibodies for various types of biosensors (Arya et al., 2007a; Kwon et al., 2006; Wang et al., 2003). Their biological and organic properties can be easily manipulated via changing functional groups that become compatible for biomolecules and are known to orient these biomolecules without denaturization (Arya et al., 2006, 2007b). Further, use of SAM and covalent binding provides options for strong and stable immobilization of a biomolecule in the very near vicinity of the sensor surface (Arya et al., 2007a; Mizutani, 2008; Yu et al., 2006). In earlier work we have shown that use of thiol molecule (dithiobis (succinimidyl propionate) (DTSP) with amine reactive succinimidyl group results in reliable SAM with facile covalent binding of enzyme, antibody and phages via amide bond formation (Arya et al., 2010, 2007a, 2011). In present work, use of succinimidyl 6-(3-[2-pyridyldithio]-propionamido) hexanoate (LC-SPDP) has been described for the first time for covalent immobilization of anti-EpCAM antibody on gold microelectrodes. Longer chain length of LC-SPDP over DTSP helps to make more uniform and aligned SAM. Further, the longer chain length helps to keep reactive succinimidyl group slightly away from the surface, thus preventing hindrance from 2-mercapto pyridine during biomolecule immobilization. Use of LC-SPDP results in the formation of mixed SAM of succinimidyl 6-(3-mercapto propionamido)-hexanoate and 2-mercapto pyridine via chemisorption on gold surface. Succinimidyl group in succinimidyl 6-(3-mercapto propionamido)hexanoate is capable of reacting with the NH_2 group biomolecules even at 4 °C and at the blood pH, resulting covalent immobilization of biomolecules, while 2-mercapto pyridine provides spacing between biomolecules and provides conductive path for charge flow from solution to electrode surface.

In present work, LC-SPDP SAM has been used for the first time to covalently immobilize anti-EpCAM for capture of breast cancer specific MCF-7 cells. Ethanol amine (EA) has been used as the surface blocking layer to prevent the non-specific binding and to remove physically adsorbed antibodies on electrode surface (Arya et al., 2010, 2011). MCF-7 cell capture and estimation on anti-EpCAM/LC-SPDP/Au electrodes have been achieved using cyclic voltammetry. Further, attempts have been made to use magnetic nanoparticles conjugated with ferrocene amidopentyl carboxylic acid tagged anti-EpCAM for molecular profiling of cells on blank gold microelectrodes. Magnetic bead based labeling can also be used for enriching the cells via immunomagnetic enrichment, thus offering a unified solution for CTC enrichment and detection.

2. Material and methods

2.1. Chemicals and reagents

Succinimidyl 6-(3-[2-pyridyldithio]-propionamido) hexanoate (LC-SPDP) (cat # C1117) was procured from proteochem, Epithelial VU-1D9 antibody (anti-EpCAM) (cat # 01420), and dextran coated magnetic particles were from Stemcell Technologies Inc. (Vancouver, Canada), ferrocene amidopentyl carboxylic acid succinimidyl ester (FeCOOH-NHS) (cat # AF0403-5) was from biotech Gmbh. 1, 4-Dioxane anhydrous (cat # 296309) was from Sigma. Phosphate buffer solution (PBS, pH 7.4) was from Invitrogen, USA. MCF-7 cells, from a human breast cancer tumor, were purchased from the American Type Culture Collection (ATCC) (cat # HTB-22) and received as frozen vials. All other chemicals were of biology grade and used without purification.

The MCF-7 cells were cultured in Gibco® Minimum Essential Media supplemented with 10% fetal bovine serum (Gibco, cat # 16000044), 1% Sodium pyruvate (Gibco, cat # 11360070), 1% MEM non-essential amino acids (Gibco, cat # 11140050), and 1% penicillin–streptomycin (Gibco, cat # 15140122). The cells were incubated in a 37 °C CO_2 incubator, upon confluency, the cells are dislodged with 1x trypsin (Gibco, cat # 25300054). The cell suspension was centrifuged at 1500 rpm for 5 min and the resultant cell pellet was resuspended in 1x PBS (Gibco, cat # 10010049). After that, the cell concentration was determined by cell counting using improved Neubauer haemocytometer and further diluted with 1x PBS for different concentrations.

2.2. Microelectrode fabrication

Microelectrodes with varying sensing areas (Fig. 1) were fabricated on glass wafer using standard micro-fabrication techniques. Titanium (Ti; 0.1 μm)/ gold (Au; 1 μm) film stack was deposited on the glass wafers using electron-beam evaporator (Temescal Inc). Ti layer acts as the adhesion promoter for the gold film. The sensing microelectrodes, bond pads, and connecting route lines were patterned by a series of processes involving photoresist spin coating (PFI-A26, Sumitomo Chemical Co., Ltd.), photolithography through a chrome mask in EVG 6200 Mask Aligner (EVG Group), and photoresist development in Shipley MF-319 developer (MicroChem Corp.). The unpatterned metal regions were etched with acid: Au etchant (Au-600, CLC) for the top Au film, and Ti etchant (Ti-890, CLC) for the adhesion Ti layer. The photoresist was stripped in solvent and the wafers were cleaned in H_2SO_4:H_2O_2 solution (3:1) at 125 °C to remove residual polymer contamination. Subsequently, the wafer was passivated with a moisture barrier layers of SiO_2 (0.8 μm)/Si_3N_4 (0.2 μm thick) through plasma enhanced chemical vapor deposition (PECVD). PECVD was conducted at 200 °C to prevent inter-diffusion of Ti into the Au surface. The sensing microelectrodes array and bond pads were exposed for electrochemical analysis after photolithography and reactive ion etching (RIE) with CF_4. The fabricated gold microelectrodes were characterized for resistance and found to possess sheet resistance of 3.5 μΩ cm.

2.3. LC-SPDP self-assembled monolayer (SAM) formation and immobilization of anti-EpCAM antibodies

The microelectrodes were pre-cleaned with acetone, ethanol, and with copious amount of de-ionized water. Further, gold microelectrodes were cleaned with piranha solution (H_2SO_4:H_2O_2; 7:3) for 5 min followed by rinsing in de-ionized water and drying in nitrogen. These gold microelectrodes were immersed into a 0.5 mg ml^{-1} solution of LC-SPDP in 1,4-dioxane overnight at room temperature for formation of mixed SAM of succinimidyl 6-(3-mercapto propionamido)hexanoate and 2-mercapto pyridine (Fig. 1a). It is a common practice to reduce disulfide bond before SAM formation onto gold, however, it is not necessary (Noh and Hara, 2001; Ulman, 1996) and is done mainly in case of proteins or when short time is used for SAM formation. In present case SAM was made via overnight incubation and pre-reduction was avoided to prevent hydrolysis or damage of reactive succinimidyl group on

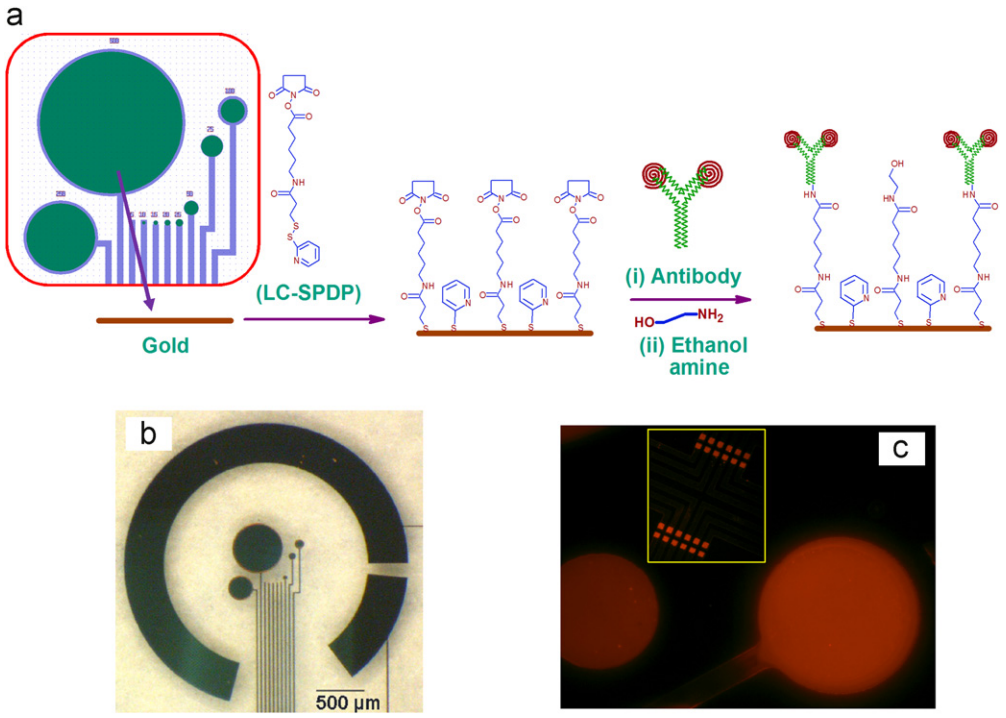

Fig. 1. (a) Schematic of microelectrodes of various sizes and fabrication of anti-EpCAM/LC-SPDP/Au electrode. (b) Optical image of blank microelectrodes. (c) Fluorescent image of fluorescently tagged antibody modified microelectrodes, (inset shows the fluorescently tagged antibody modified $25 \times 25\ \mu m^2$ electrode array).

LC-SPDP over long time of incubation. Succinimidyl group in succinimidyl 6-(3-mercapto propionamido) hexanoate was used for covalent immobilization of anti-EpCAM and 2-mercapto pyridine created spacing between amine reactive succinimidyl groups in mixed SAM and provided conductive path for charge flow from solution to electrode surface. After the SAM formation, microelectrodes were rinsed with 1,4-dioxane and acetone to remove any unbound LC-SPDP followed by rinsing in water and drying under nitrogen gas. The LC-SPDP modified electrodes after their preparation were utilized immediately for immobilization of anti-EpCAM.

Anti-EpCAM antibodies were covalently attached to LC-SPDP self-assembled monolayer by incubating the electrode in 1 μl of 1 mg ml^{-1} antibody solution for 1.5 h in humid chamber. Covalent binding via amide bond formation results from the facile reaction between amino group of antibody and reactive succinimidyl group of the LC-SPDP on the SAM surface (Fig. 1a). The sensor (anti-EpCAM/LC-SPDP/Au) was washed thoroughly with phosphate buffer (10 mM, pH 7.4) to remove any unbound antibodies followed by a 10 min washing with 1% ethanol amine solution in PBS. Ethanol amine as blocker was used to block unreacted succinimidyl group on LC-SPDP SAM and to remove extra unbound antibodies onto the electrode surface. The electrodes were stored at 4 °C while not in use. The fabricated anti-EpCAM/LC-SPDP/Au electrodes were characterized using the optical and cyclic voltammetric techniques, respectively.

2.4. Optical and cyclic voltammetry (CV) studies of microelectrodes

For optical characterization, picture for fabricated microelectrode chip was taken using Olympus U-TV0.5X microscope fitted with Sony's Exwave HAD color video camera. Fluorescence image for fluorescently tagged anti-EpCAM immobilized on LC-SPDP SAM was recorded using Olympus BX61 fluorescence microscope fitted with cooled digital CCD camera from RTKE Diagnostic Instruments Inc. For CV characterization, cyclic voltammetry was performed on an Autolab Potentiostat/Galvanostat (Eco Chemie, Netherlands) using a three-electrode configuration with on-chip gold electrode as a pseudo reference and counter electrode in 10 μl of phosphate buffer saline (PBS) solution (1x, pH 7.4) containing mixture of 10 mM $Fe(CN)_6^{4-}$ (ferrocyanide) and 10 mM of $Fe(CN)_6^{3-}$ (ferricyanide) i.e. 10 mM $Fe(CN)_6^{3-/4-}$ as a redox probe. For molecular profiling CV was performed in10 μl of PBS solution (1x, pH 7.4,) in similar three-electrode setup. For CV data recording, measurements were carried out from −0.7 to 0.7 V at scan rate of 4 V s^{-1}.

2.5. Cell capturing studies

For specific capture of breast cancer specific MCF-7 cells, 1 μl of MCF-7 cell suspensions in PBS with desired concentrations was loaded onto the chips and kept at room temperature for 15 min. During this time, cells were allowed to interact with surface bound anti-EpCAM for specific cells capture via standard antibody–antigen binding based chemistry. After cell capture, chip was washed gently with PBS to remove extra unbounded cells. Cell capture was studied using CV technique and used for detection range estimation.

2.6. Molecular profiling of MCF-7 cells via magnetic beads conjugated to redox tagged antibodies

To differentiate the cancerous cells from normal cells, cell profiling for surface markers can provide valuable information and can be utilized to identify cell type. MCF-7 cells expressing high level of EpCAM on their surface were identified by testing them on 500 μm (diameter) and 50 μm (diameter) size blank gold microelectrodes after tagging with magnetic beads conjugated to ferrocene amidopentyl carboxylic acid modified anti-EpCAM (MagB–anti-EpCAM-FeCOOH). For each measurement only desired size electrode was used as working electrode.

2.6.1. Tagging of anti-EpCAM

FeCOOH tagging to anti-EpCAM was achieved via incubation of 100 μl of 0.5 mg ml^{-1} anti-EpCAM with 8 μl of borate buffer

(0.67 M) and 0.2 mg of FeCOOH-NHS in DMSO for 1 h at room temperature followed by overnight incubation at 4 °C before use. FeCOOH tagged anti-EpCAM was then used for further conjugation with dextran coated magnetic beads via incubation of tagged anti-EpCAM with magnetic beads in 1:2 for 15 min at room temperature followed by magnetic collection of beads and washing with PBS twice to remove extra anti-EpCAM-FeCOOH.

2.6.2. Tagging of MCF-7 cells with tagged anti-EpCAM

MCF-7 cell tagging with MagB-FeCOOH-anti-EpCAM, 5 µl FeCOOH-anti-EpCAM tagged to 10 µl magnetic beads was incubated with 1 ml of 10^6 MCF-7 cells for 30 min at 4 °C, followed by collecting cells by centrifugation at 1500 rpm for 5 min and resuspending in fresh PBS to remove extra unbound antibodies. Centrifugation and resuspention were repeated two times before final centrifugation and desired concuntration of cells makeup in PBS.

3. Results and discussions

3.1. Optical characterization for anti-EpCAM/LC-SPDP/Au electrodes fabrication

Fig. 1b and c shows the optical and fluorescent image of blank microelectrodes and fluorescently tagged antibodies immobilized on LC-SPDP SAM, respectively. The exposed circular area covered by a ring in Fig. 1b represents the active gold area as all other areas including connection wires are covered with insulating SiO_2/Si_3N_4 layer and do not contribute to any signal. Bright and uniform fluorescence visible in Fig. 1c confirms the dense and uniform binding of antibodies. Inset in Fig. 1c shows the fluorescence image of fluorescently tagged antibodies immobilized on LC-SPDP modified $25 \times 25\ \mu m^2$ electrodes indicating that binding via described procedure also result in uniform antibody binding even on very small size microelectrodes.

3.2. Cyclic voltammetric characterization for anti-EpCAM/LC-SPDP/Au electrodes fabrication

Anti-EpCAM/LC-SPDP/Au electrode fabrication was characterized at each step of modification using CV measurement in the range of −0.7–0.7 V at $4\ s^{-1}$. Fig. 2 shows the CV spectra recorded for: (i) blank Au, (ii) LC-SPDP/Au, (iii) anti-EpCAM/LC-SPDP/Au, and (iv) 1% ethanol amine (EA) treated anti-EpCAM/LC-SPDP/Au electrode of 500 µm (diameter). In curve (ii), the dramatic decrease in the oxidation current for LC-SPDP/Au electrode compared to that of the Au electrode (curve (i)), indicates the formation of LC-SPDP SAM, which results in some insulation on gold surface and decreases the electron transport during oxidation and reduction. The further reduction in the oxidation current in CV for anti-EpCAM/LC-SPDP/Au electrode (curve (iii)) on anti-EpCAM binding confirms the immobilization of antibodies. In curve (iv) after the treatment with EA slight increase in oxidation current was observed, which can be attributed to the removal of unbound insulating antibodies.(Arya et al., 2010, 2011). These observed changes at each step of indicating successful modification of microelectrode.

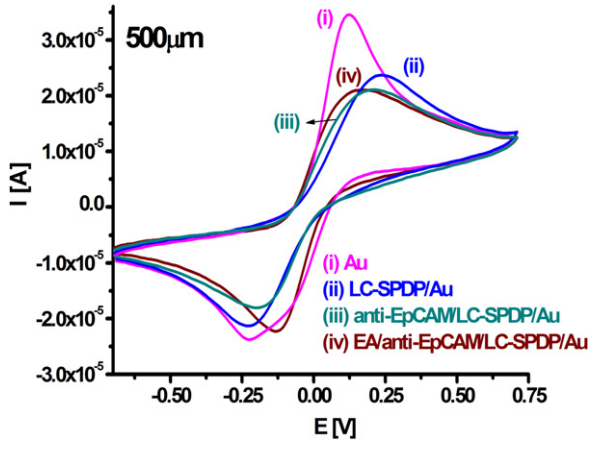

Fig. 2. CV spectra for: (i) Au surface, (ii) LC-SPDP/Au, (iii) anti-EpCAM/LC-SPDP/Au, and (iv) EA treated anti-EpCAM/LC-SPDP/Au electrode of 500 µm (diameter) in three-electrode configuration with on-chip gold electrode as a pseudo reference and counter electrode in PBS solution (1x, pH 7.4) containing 10 mM $Fe(CN)_6^{3-/4-}$ as a redox probe.

3.3. CV studies for MCF-7 cell detection

MCF-7 cells concentration effect from 1×10^5 to 1×10^8 cells ml^{-1} range was studied on 500 µm (diameter) EA treated anti-EpCAM/LC-SPDP/Au electrodes via CV from −0.7 to 0.7 V in PBS containing10 mM $Fe(CN)_6^{3-/4-}$. Fig. 3a shows the CV spectra of EA treated anti-EpCAM/LC-SPDP/Au electrodes as a function of MCF-7 concentrations. The decrease in value of peak current with increase in MCF-7 cells concentration indicates more and more coverage of electrode surface by specifically captured cells. Fig. 3b showing absolute value of peak current obtained from different concentration without base line correction reveals that the EA treated anti-EpCAM/LC-SPDP/Au electrode can be used to estimate MCF-7 cells from 1×10^5 to 1×10^8 cells ml^{-1}

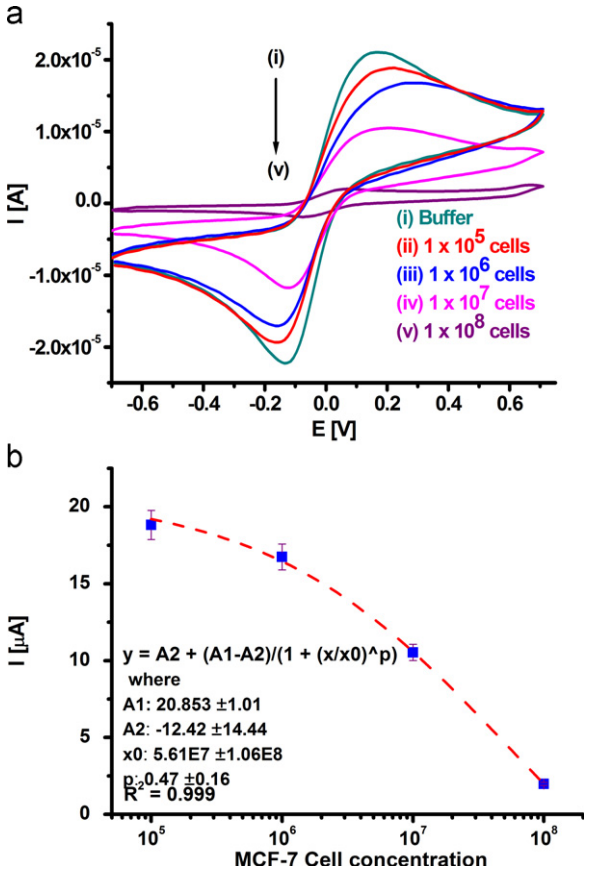

Fig. 3. (a) CV spectra of EA treated anti-EpCAM/LC-SPDP/Au electrodes as a function of MCF-7 concentrations: (i) 0 cells ml^{-1}, (ii) 1×10^5 cells ml^{-1}, (iii) 1×10^6 cells ml^{-1}, (iv) 1×10^7 cells ml^{-1}, and (v) 1×10^8 cells ml^{-1} for 500 µm (diameter) electrode in three-electrode configuration with on-chip gold electrode as a pseudo reference and counter electrode in PBS solution (1x, pH 7.4) containing 10 mM $Fe(CN)_6^{3-/4-}$ as a redox probe. (b) Plot of peak current response versus MCF-7 concentrations and sigmoidal fitting.

range and perfectly follow sigmoidal fit. The results of triplicate sets (shown as error bars) reveal the reproducibility to be within a 5% error. Electrode exhibits correlation coefficient of 0.999, standard deviation of 0.5 μA, and detection limit of 1×10^5 cells ml^{-1} i.e. 100 cells in solution used for incubation (1 μl). Further, very small CV signal change was observed for anti-EpCAM/LC-SPDP/A electrode when tested for jurkat cells (1×10^6 cells ml^{-1}) (Fig. 4), thus suggesting the specificity of fabricated electrode.

3.4. Cell identification via specific recognition using magnetic beads conjugated to redox tagged antibodies

To differentiate the cancerous cells from normal cells, cell profiling for surface markers was carried out to identify cell. MCF-7 cells were tested via CV in PBS on blank 500 μm (diameter) and 50 μm (diameter) electrodes surface to identify surface marker on them. Pure cultured MCF-7 cells were first tested on blank microelectrode and then compared with cells tagged with MagB–anti-EpCAM-FeCOOH. For testing 1 μl of tagged or untagged cells was poured onto the working microelectrodes and concentrated on active area using patch clamp setup (World Precision Instruments, USA) and kept in air for 15 min to settle down on desired electrode, after which 10 μl of PBS was poured on chip and CV measurements were recorded in three-electrode configuration.

Fig. 5 shows the CV spectra of 500 μm (diameter) electrode with: (i) no cells, (ii) with pure MCF-7 cells, and (iii) with MagB-anti-EpCAM-FeCOOH tagged MCF-7 cells. It is clear from figure that current decreases in presence of cells; however, from this decrease one cannot define the cell type. In CV spectra for MagB-anti-EpCAM-FeCOOH tagged MCF-7 cells (curve (iii)) a new broad band near 0.28 V was appeared. This new band can be attributed to the presence of ferrocene molecules on the cell surface, thus indicating the presence of anti-EpCAM specific proteins on cell surface. This presence of anti-EpCAM specific proteins on cell surface can be utilized to distinguish and confirm the cancerous nature of cell over normal blood cells. Cell identification experiment was performed number of times in triplicate sets. Each time new band for ferrocene was observed, however, variation of more than 10% was observed in peak current, which can be attributed to the varying number of redox tagged magnetic particle binding onto the cell and contributing toward signal. Thus, signal can be used for identification of cell but not for quantification of surface marker concentration.

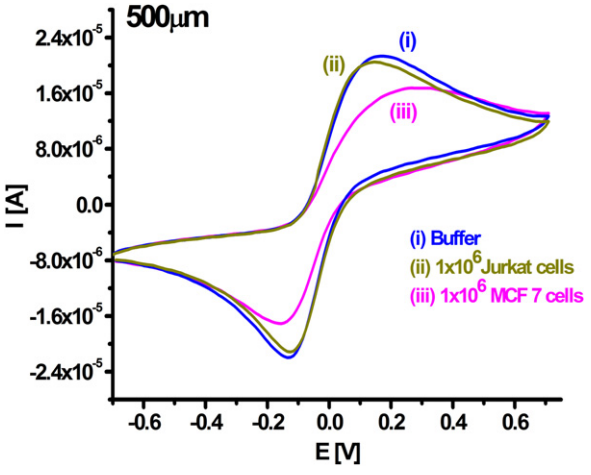

Fig. 4. CV spectra of EA treated anti-EpCAM/LC-SPDP/Au electrodes as a function of: (i) buffer, (ii) jurkat cells (1×10^6), and (iii) MCF-7 cells (1×10^6) for 500 μm (diameter) electrode in three-electrode configuration with on-chip gold electrode as a pseudo reference and counter electrode in PBS solution (1x, pH 7.4) containing 10 mM $Fe(CN)_6^{3-/4-}$ as a redox probe.

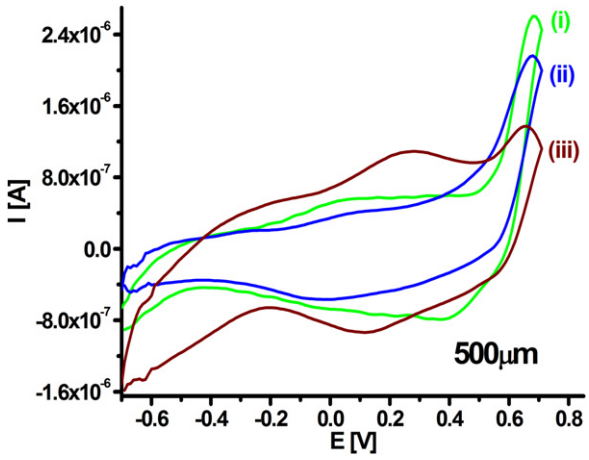

Fig. 5. CV spectra of 500 μm (diameter) electrode with: (i) no cells, (ii) with pure MCF-7 cells, and (iii) with MagB-anti-EpCAM-FeCOOH tagged MCF-7 cells in three-electrode configuration with on-chip gold electrode as a pseudo reference and counter electrode in PBS solution (1x, pH 7.4).

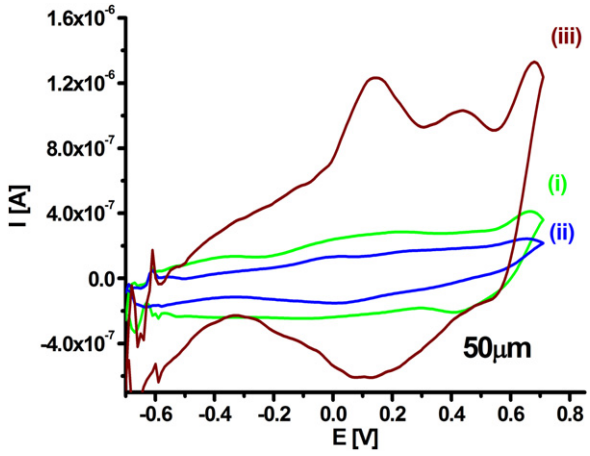

Fig. 6. CV spectra of 50 μm (diameter) electrode with: (i) no cells, (ii) with pure MCF-7 cells, and (iii) with MagB-anti-EpCAM-FeCOOH tagged MCF-7 cells in three-electrode configuration with on-chip gold electrode as a pseudo reference and counter electrode in PBS solution (1x, pH 7.4).

For higher sensitivity and better resolution cell identification experiments were repeated on 50 μm (diameter) electrodes. Fig. 6 shows the CV spectra of 50 μm (diameter) electrode with: (i) no cells, (ii) with pure MCF-7 cells, and (iii) with MagB-anti-EpCAM-FeCOOH tagged MCF-7 cells. Decrease in current after cell loading in curve (ii) was found to be more prominent compared to 500 μm (diameter) electrode and indicates the presence of cells over electrode surface. In CV spectra for MagB-anti-EpCAM-FeCOOH tagged MCF-7 cells (curve (iii)) appearance of well-defined and prominent new peak near 0.41 V for FeCOOH suggest the successful tagging of cells with FeCOOH tagged antibodies. Further, it confirms the presence of EpCAM on cell surface which is the indication of tumorous cells presence. Reason for appearance of 2nd peak near 0.18 V is not clear and further experiments are under investigation for understanding. Presence of well-defined and prominent peak at 0.41 V in 50 μm (diameter) electrode suggest higher resolution and the advantage of smaller microelectrode in cell profiling with better sensitivity. Similar to earlier experiments, cell identification experiment on 50 μm

(diameter) electrodes was performed number of times in triplicate sets. Each time more prominent peak near 0.41 V for FeCOOH compared to 500 μm (diameter) electrode was observed, however, variation of more than 7% was observed in peak current, which can again be attributed to the varying number of magnetic particle binding onto the cell and contributing toward signal. Thus, even in smaller electrodes signal for FeCOOH can be used for identification of cell but not for quantification of surface marker concentration. Based on these results, it can be hypothesized that use of high density array of smaller and individually addressable electrodes with mixture of antibodies tagged with different redox tag can be employed for high throughput tumor cell screening and profiling. Further, the use of magnetic bead based labeling can also be used for enriching the cells via immunomagnetic enrichment, thus offering a unified solution for CTC enrichment and detection.

4. Conclusion

In present work LC-SPDP SAM prepared on microelectrodes has been used for the first time to covalently immobilize anti-EpCAM for specific capture of breast cancer specific MCF-7 cells. For biosensor fabrication, amino group on anti-EpCAM antibody was covalently bound with succinimidyl group on SAM via amide bond and unreacted active groups of LC-SPDP were blocked using 1% ethanol amine (EA). CV results for anti-EpCAM/LC-SPDP/Au electrodes exposed to solutions with different MCF-7 cell concentrations reveal the detection of MCF-7 cells in the range of 1×10^5–1×10^8 cells ml^{-1} with correlation coefficient of 0.999 and detection limit of 1×10^5 cells ml^{-1} i.e. 100 cells in solution used for incubation (1 μl). Cancer cell identification via molecular profiling of cells on microelectrodes using ferrocene amidopentyl carboxylic acid based redox tagging and magnetic beads based enhancement was achieved by CV investigation in PBS. Results suggested that 50 μm (diameter) microelectrodes are better for molecular profiling. In future, attempts should be made to use mixture of antibodies tagged with different redox probes for multi marker identification on high density smaller sized microelectrode array for screening, enumeration, and more specific identification of cancer cell type. Moreover, attempts should be made to use such tagged magnetic bead for enriching the cells via immunomagnetic enrichment and profiling simultaneously for unified solution for CTC enrichment and identification.

Acknowledgments

The authors would like to thank and acknowledge funding provided by A*STAR (Agency for Science, Technology and Research), Singapore.

References

Adams, A.A., Okagbare, P.I., Feng, J., Hupert, M.L., Patterson, D., Gottert, J., McCarley, R.L., Nikitopoulos, D., Murphy, M.C., Soper, S.A., 2008. Journal of the American Chemical Society 130, 8633–8641.
Alunni-Fabbroni, M., Sandri, M.T., 2010. Methods 50, 289–297.
Amadori, A., Rossi, E., Zamarchi, R., Carli, P., Pastorelli, D., Jirillo, A., 2009. Oncology 76, 375–386.
Arya, S.K., Chornokur, G., Venugopal, M., Bhansali, S., 2010. Biosensors & Bioelectronics 25, 2296–2301.
Arya, S.K., Lee, K.C., Dahalan, D.B., Daniel, Rahman, A.R.A., 2012. Lab on a Chip 12, 2362–2368.
Arya, S.K., Pandey, P., Singh, S.P., Datta, M., Malhotra, B.D., 2007a. Analyst 132, 1005–1009.
Arya, S.K., Singh, A., Naidoo, R., Wu, P., McDermott, M.T., Evoy, S., 2011. Analyst 136, 486–492.
Arya, S.K., Solanki, P.R., Singh, R.P., Pandey, M.K., Datta, M., Malhotra, B.D., 2006. Talanta 69, 918–926.
Arya, S.K., Solanki, P.R., Singh, S.P., Kaneto, K., Pandey, M.K., Datta, M., Malhotra, B.D., 2007b. Biosensors & Bioelectronics 22, 2516–2524.
Braun, S., Marth, C., 2004. New England Journal of Medicine 351, 824–826.
Chung, Y.K., Reboud, J., Lee, K.C., Lim, H.M., Lim, P.Y., Wang, K.Y., Tang, K.C., Ji, H., Chen, Y., 2011. Biosensors & Bioelectronics 26, 2520–2526.
Cristofanilli, M., Budd, G.T., Ellis, M.J., Stopeck, A., Matera, J., Miller, M.C., Reuben, J.M., Doyle, G.V., Allard, W.J., Terstappen, L.W.M.M., Hayes, D.F., 2004. New England Journal of Medicine 351, 781–791.
Davies, T.J., Compton, R.G., 2005. Journal Of Electroanalytical Chemistry 585, 63–82.
De Bono, J.S., Scher, H.I., Montgomery, R.B., Parker, C., Miller, M.C., Tissing, H., Doyle, G.V., Terstappen, L.W.W.M., Pienta, K.J., Raghavan, D., 2008. Clinical Cancer Research 14, 6302–6309.
De la Rica, R., Thompson, S., Baldi, A., Fernandez-Sanchez, C., Drain, C.M., Matsui, H., 2009. Analytical Chemistry 81, 10167–10171.
Gaforio, J.J., Serrano, M.-J., Sanchez-Rovira, P., Sirvent, A., Delgado-Rodriguez, M., Campos, M., De la Torre, N., Algarra, I., Duenas, R., Lozano, A., 2003. International Journal of Cancer 107, 984–990.
Hosokawa, M., Hayata, T., Fukuda, Y., Arakaki, A., Yoshino, T., Tanaka, T., Matsunaga, T., 2010. Analytical Chemistry 82, 6629–6635.
Issadore, D., Shao, H., Chung, J., Newton, A., Pittet, M., Weissleder, R., Lee, H., 2011. Lab on a Chip 11, 147–151.
Krishnamurthy, S., Cristofanilli, M., Singh, B., Reuben, J., Gao, H., Cohen, E.N., Andreopoulou, E., Hall, C.S., Lodhi, A., Jackson, S., Lucci, A., 2010. Cancer 116, 3330–3337.
Kuo, J.S., Zhao, Y., Schiro, P.G., Ng, L., Lim, D.S.W., Shelby, J.P., Chiu, D.T., 2010. Lab on a Chip 10, 837–842.
Kwon, S.J., Kim, E., Yang, H., Kwak, J., 2006. Analyst 131, 402–406.
Li, H., Wei, Q., He, J., Li, T., Zhao, Y., Cai, Y., Du, B., Qian, Z., Yang, M., 2011. Biosensors & Bioelectronics 26, 3590–3595.
Li, T., Fan, Q., Liu, T., Zhu, X., Zhao, J., Li, G., 2010. Biosensors & Bioelectronics 25, 2686–2689.
Lin, H.K., Zheng, S., Williams, A.J., Balic, M., Groshen, S., Scher, H.I., Fleisher, M., Stadler, W., Datar, R.H., Tai, Y.-C., Cote, R.J., 2010. Clinical Cancer Research 16, 5011–5018.
Miller, M.C., Doyle, G.V., Terstappen, L.W.M.M., 2010. Journal of Oncology, 2010.
Mizutani, F., 2008. Sensors & Actuators B 130, 14–20.
Moon, H.S., Kwon, K., Kim, S.I., Han, H., Sohn, J., Lee, S., Jung, H.I., 2011. Lab on a Chip 11, 1118–1125.
Mostert, B., Sleijfer, S., Foekens, J.A., Gratama, J.W., 2009. Cancer Treatment Reviews 35, 463–474.
Noh, J., Hara, M., 2001. Focused on Nanotechnology in RIKEN I 37, 54–57.
Ordeig, O., Banks, C.E., Davies, T.J., Del Campo, J., Mas, R., Munoz, F.X., Compton, R.G., 2006. Analyst 131, 440–445.
Pantel, K., Riethdorf, S., 2009. Nature Reviews Clinical Oncology 6, 190–191.
Rahman, A., Guiseppi-Elie, A., 2009. Biomedical Microdevices 11, 701–710.
Rahman, A.R.A., Lo, C.M., Bhansali, S., 2009. IEEE Transactions on Biomedical Engineering 56, 485–492.
Riethdorf, S., Fritsche, H., Muller, V., Rau, T., Schindlbeck, C., Rack, B., Janni, W., Coith, C., Beck, K., Jänicke, F., Jackson, S., Gornet, T., Cristofanilli, M., Pantel, K., 2007. Clinical Cancer Research 13, 920–928.
Ring, A., Smith, I.E., Dowsett, M., 2004. The Lancet Oncology 5, 79–88.
Ross, J.S., Slodkowska, E.A., 2009. American Journal of Clinical Pathology 132, 237–245.
Sequist, L.V., Nagrath, S., Toner, M., Haber, D.A., Lynch, T.J., 2009. Journal of Thoracic Oncology 4, 281–283.
Slade, M.J., Coombes, R.C., 2007. Nature Clinical Practice Oncology 4, 30–41.
Sun, Y.F., Yang, X.R., Zhou, J., Qiu, S.J., Fan, J., Xu, Y., 2011. Journal of Cancer Research 137, 1151–1173.
Tan, S., Yobas, L., Lee, G., Ong, C., Lim, C., 2009. Biomedical Microdevices 11, 883–892.
Ulman, A., 1996. Chemical Reviews 96, 1533–1554.
Wang, M., Sun, C., Wang, L., Ji, X., Bai, Y., Li, T., Li, J., 2003. Journal of Pharmaceutical and Biomedical Analysis 33, 1117–1125.
Yu, X., Lv, R., Ma, Z., Liu, Z., Hao, Y., Li, Q., Xu, D., 2006. Analyst 131, 745–750.
Zborowski, M., Chalmers, J.J., 2011. Analytical Chemistry 83, 8050–8056.
Zheng, S., Lin, H., Lu, B., Williams, A., Datar, R., Cote, R., Tai, Y.C., 2011a. Biomedical Microdevices 13, 203–213.
Zheng, X., Cheung, L.S.L., Schroeder, J.A., Jiang, L., Zohar, Y., 2011b. Lab on a Chip 11, 3269–3276.